

BOTTOM PARAMETERS INVERSION VIA BAYESIAN THEORY IN THE DEEP OCEAN

Xiaole Guo^{a,b}, Kunde Yang^{a,b}, Rui Duan^{a,b}, Yuanliang Ma^{a,b}

^aSchool of Marine Science and Technology, Northwestern Polytechnical University, Xi'an 710072

^bKey Laboratory of Ocean Acoustics and Sensing (Ministry of Industry and Information Technology), Northwestern Polytechnical University, Xi'an 710072

Contact author's name: Kunde Yang.

Complete postal address: 127 West Youyi Road Xi'an Shaanxi, 710072, P.R.China.

Email address: ykdzym@nwpu.edu.cn; lexg@mail.nwpu.edu.cn.

Abstract: *This paper develops a new approach to estimating bottom parameters based on Bayesian theory in the deep ocean. The solution in a Bayesian inversion is characterized by its posterior probability density (PPD), which combines prior information about the model with information from an observed data set. Bottom parameters are sensitive to the transmission loss (TL) data in the shadow zone of the deep ocean. In this study, TLs of different frequencies from the South China Sea (SCS) in the summer of 2014 are used as observed data sets. The interpretation of the multidimensional PPD requires the calculation of its moments, such as the mean, covariance, and marginal distributions, which provide parameter estimates and uncertainties. Considering that the sensitivities of shallow-zone TLs vary for different frequencies of the bottom parameters in the deep ocean, this research obtained bottom parameters at varying frequencies. Then, the inversion results compare with the sampling data. Besides, this paper shows the inversion results for multi-frequency combined inversion.*

Keywords: *Geoacoustic inversion, Bayesian theory, deep ocean*

1. INTRODUCTION

The problem of determining bottom parameters from measured ocean acoustic fields has received considerable attention in recent years[1-5]. With the development of underwater acoustics from shallow water to the deep ocean, bottom parameter inversion in the deep ocean needs to be researched more thoroughly. Geoacoustic inversion represents a strongly nonlinear inverse problem for which a direct solution is unavailable. For nonlinear problems, Gaussian data uncertainties do not imply Gaussian parameter uncertainties, and no general analytic solution is available. However, Bayesian inference theory provides a formalism for estimating parameter uncertainties for nonlinear inverse problems[6,7]. In a Bayesian formulation, the solution to inversion problem is characterized by the PPD of the unknown model parameters. The PPD combines prior information about the model with the information provided by an observed data set. The data information is expressed in terms of the likelihood function defined by the statistical distribution of data errors. To interpret the multidimensional PPD in a useful manner, the state of information about the model parameters is typically quantified in terms of moments of the PPD, such as the posterior mean, marginal probability distributions (MPD), and covariances, which provide parameter estimates and uncertainties. Good overviews of the application of Bayesian inference to geophysical inverse problems are given by Tarantola[8] and Sen and Stoffa[9,10].

In this study, the TL of the shadow zone obtained in the experiment is used as the observed data set. The bottom is assumed to be a two-layered bottom model. This research used Bayesian theory to obtain the bottom parameters of different frequencies. The inverted bottom parameters of different frequencies have a certain difference. The main reason is that the inversion results are equivalent results under the corresponding frequency. Besides, this paper shows the inversion results for multi-frequency combined inversion. Finally, the inversion results are validated using the experimental TLs and the numerical results, which are calculated through the inverted bottom parameters for varying source depths and receiver depths at the corresponding frequency.

2. BASIC THEORY

In this study, the TL data, which are obtained in a deep ocean experiment conducted in the SCS, are the observed vectors \mathbf{d}^e . The numerical TL data, which are calculated by RAM model, are the model vectors \mathbf{m} . Bayes' rule, which follows from the definition of conditional probabilities, may be expressed as

$$P(\mathbf{m} | \mathbf{d}^e) = \frac{P(\mathbf{d}^e | \mathbf{m})P(\mathbf{m})}{P(\mathbf{d}^e)} \quad (1)$$

where $P(\mathbf{m} | \mathbf{d}^e)$ represents the conditional probability density function (PDF) of \mathbf{m} for given \mathbf{d}^e , $P(\mathbf{d}^e | \mathbf{m})$ is the conditional PDF of \mathbf{d}^e for given \mathbf{m} , $P(\mathbf{m})$ is the PDF of independent of \mathbf{d}^e , and $P(\mathbf{d}^e)$ is the PDF of \mathbf{d}^e . Considering that the denominator of Eq. (1) is independent of \mathbf{d}^e , Eq. (1) can be considered as a constant factor, and it can be rewritten as $P(\mathbf{m} | \mathbf{d}^e) \propto P(\mathbf{d}^e | \mathbf{m})P(\mathbf{m})$. During this inversion, $P(\mathbf{d}^e | \mathbf{m})$ is regarded as

the likelihood function $L(\mathbf{d}^e | \mathbf{m})$, which represents the information provided by the TLs. Thus, Eq. (1) becomes $P(\mathbf{m} | \mathbf{d}^e) \propto L(\mathbf{d}^e | \mathbf{m})P(\mathbf{m})$. The likelihood function $L(\mathbf{d}^e | \mathbf{m})$ is determined by the form of the observed data and the statistical distribution of the data errors. In practice, obtaining an independent estimate of the error statistics is often difficult, and simplifying assumptions are required to proceed. For the unbiased Gaussian errors, the likelihood function $L(\mathbf{d}^e | \mathbf{m})$ is of the form

$$L(\mathbf{d}^e | \mathbf{m}) \propto \exp[-E(\mathbf{m})] \quad (2)$$

where $E(\mathbf{m})$ represents the error function appropriate to the state of available information and can be defined as

$$E(\mathbf{m}) = \frac{1}{2} [\mathbf{d}^e - \mathbf{r}(\mathbf{m})]^* \mathbf{C}^{-1} [\mathbf{d}^e - \mathbf{r}(\mathbf{m})] \quad (3)$$

where $(\cdot)^*$ indicates conjugate transpose, $(\cdot)^{-1}$ indicates matrix inversion, $\mathbf{r}(\mathbf{m})$ is the model calculated TL for parameter vectors \mathbf{m} , and \mathbf{C} is the data error covariance. For this study, the experimental TL symbols jump randomly back and forth across the line that represents the numerical TLs. Therefore, the data errors are assumed to be unbiased Gaussian errors that are uncorrelated and have the same variance σ^2 . Consequently, Eq. (5) becomes

$$E(\mathbf{m}) = \sum_{i=1}^N \frac{[d_i^e - r_i(\mathbf{m})]^2}{2\sigma^2} \quad (4)$$

where N represents the total sample number of TL. Formally, the variance, σ^2 , is calculated by an ensemble average over many measurements, which are often not available. In this research, the variance is obtained from the observed TL, and the calculated TL for a set of initial parameter values \mathbf{m}_0 . Therefore, the variance is

$$\sigma^2 = \sum_{i=1}^N \frac{[d_i^e - r_i(\mathbf{m}_0)]^2}{N} \quad (5)$$

Based on Eqs. (2)-(5), the normalized PPD is transformed to

$$P(\mathbf{m} | \mathbf{d}^e) = \frac{\exp[-E(\mathbf{m})]}{\int \exp[-E(\mathbf{m}')] d\mathbf{m}'} \quad (6)$$

From the view of Bayesian theory, the PPD $P(\mathbf{m} | \mathbf{d}^e)$ represents the general solution to the inverse problem. However, to interpret multidimensional problems, this study computes the integral properties of the distribution, such as the posterior mean model, model covariance matrix, and MPD for parameter m_i , which are defined, respectively, as

$$P(m_i | \mathbf{d}^e) = \int \delta(m'_i - m_i) P(\mathbf{m}' | \mathbf{d}^e) d\mathbf{m}' \quad (7)$$

where δ is the Dirac delta function, and the range of integral is the space of each parameter. The uncertainty of each parameter can be given by a one-dimensional (1D) MPD.

Though the inversion results are equivalent results under the corresponding frequency, we are more willing to get a set of bottom parameters for wideband signal. Therefore, this paper presents the multi-frequency combined inversion. In this way, the error function $E(\mathbf{m})$ can be formulated as

$$E(\mathbf{m}) = \sum_{f=f_1}^{f_2} \sum_{i=1}^{N_f} \frac{[d_{f,i}^e - r_{f,i}(\mathbf{m})]^2}{2\sigma_f^2} \quad (8)$$

where N_f and σ_f^2 represent the number of sample data and the data variance of frequency f , f_1 and f_2 represent the minimum and maximum frequency of wideband signal, respectively. For frequency f , the variance, σ_f^2 , is calculated by

$$\sigma_f^2 = \sum_{i=1}^{N_f} \frac{[d_{f,i}^e - r_{f,i}(\mathbf{m}_0)]^2}{N_f} \quad (9)$$

3. EXPERIMENTAL VERIFICATION

In the summer of 2014, an experiment on sound propagation was conducted in the deep ocean area of the SCS. A vertical receiver array at the bottom comprised 16 underwater signal recorders (USR) from the depth of 110 m to 820 m. The sample rate of the hydrophones was 48 kHz, and the sensitivity of the hydrophones was -180 dB ref. 1 V/ μ Pa. The broadband explosive sources with 1 kg TNT and nominal detonation depths of 50 m and 300 m were dropped by turns from the ship away from the receiver array. Figure 1 shows the sound speed profile (SSP), which was measured using conductance-temperature-depth (CTD) during the experimental period. As shown in Fig. 1(a), the channel axis is at the depth of 1100 m, and the speed at the bottom is 1531 m/s. Figure 1(b) displays the bathymetry along the propagation track. The whole distance of the track was 160 km, and the average depth was approximately 4100 m.

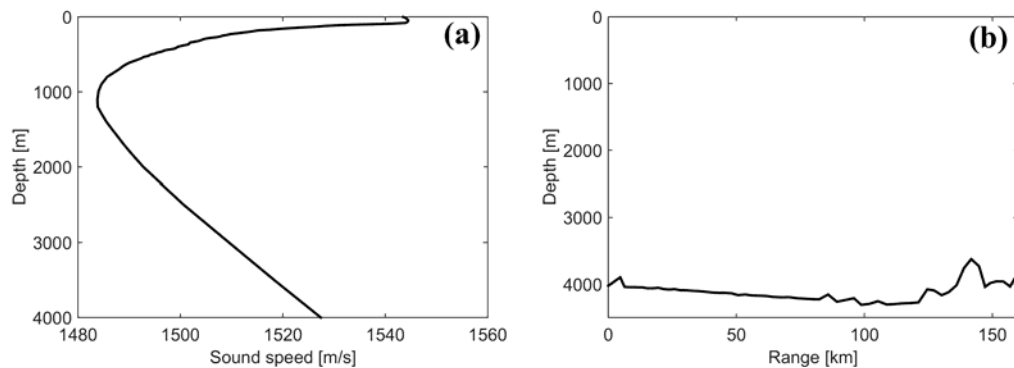


Fig.1: The conditions of marine environment.

This paper uses a two-layered bottom model to describe the environment. The RAM model is used to calculate the numerical TLs. The unknown parameters in the inversion are the sediment thickness (H), upper sediment speed (c_1), lower sediment speed (c_2), sediment density (ρ_1), sediment attenuation (α_1), basement speed (c_3), basement density (ρ_2), and basement attenuation (α_2). During the inversion, this study uses the detonation depths of 300 m sources to invert. The TL data from the USR whose depth is 177 m within the range of 20-160 km are used to invert the bottom parameters. Given that the inversion results are equivalent results under the corresponding frequency. This research calculates the TLs to invert the bottom parameters under different frequencies. Table 1 lists the inverted parameters under different frequencies and the sampling data. It shows that the inversion results have a certain difference under varying frequencies. The speed of sampling data is 1496.6 m/s, thus, the surface of bottom is a low speed bottom. The speed and density of sampling data are similar to the upper sediment speed and sediment density for all frequencies. Therefore, this research using two-layered bottom model is reasonable. To illustrate the uncertainty of inversion results under low and high frequencies, Fig. 2 provide the 1D MPDs of each parameter under 100 Hz. The inversion results are represented by the vertical lines, whereas the MPDs are depicted by the curves. Figure 2 shows the following: (a) The sediment thickness, upper sediment speed, lower sediment speed, sediment attenuation, and basement attenuation have high credibility for 100 Hz because the MPDs are sharp; and (b) the sediment density, basement speed, and basement density have low credibility because their MPDs are very wide. Furthermore, the experimental TL is consistent with the numerical TL, which is calculated using the inverted parameters for 100 Hz.

Frequency [Hz]	Layer	Thickness [m]	Speed [m/s]		Density [g/cm ³]	Attenuation [dB/ λ]
			Upper	Lower		
100	Sediment	13.8608	1486.7	1548.7	1.2965	0.1422
	Basement		1889.8		1.8596	0.2942
250	Sediment	13.2345	1506.2	1534.8	1.4198	0.1132
	Basement		1782.8		1.8246	0.2802
500	Sediment	17.2744	1493.5	1511.6	1.4273	0.0799
	Basement		1862.7		1.6077	0.2601
1000	Sediment	17.3279	1491	1592	1.4697	0.0741
	Basement		1803.6		1.8931	0.5718
Sampling data			1496.6		1.39	

Table 1: Inversion results under different frequencies.

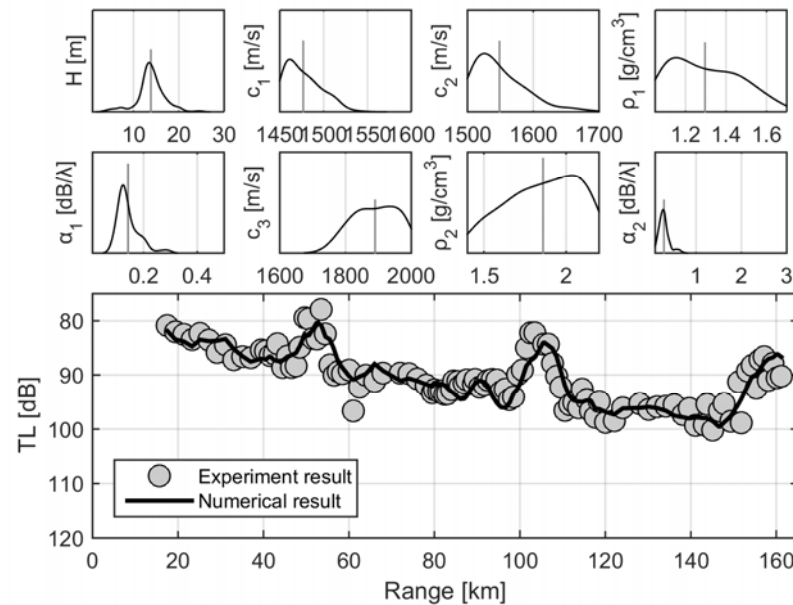


Fig.2: 1D MPDs of each parameter and the TL for inversion results under 100 Hz.

In order to obtain the inversion results for wideband signal. This paper combines 100 Hz, 250 Hz, 500 Hz and 1000 Hz to invert the bottom parameters in multi-frequency combined inversion. Table 2 lists the inversion results. The upper sediment speed is 1503.9 m/s, which is similar to the speed of sampling data. There are certain differences between the results of multi-frequency combined inversion and the results of single frequency inversion. Figure 3 exhibits the 1D MPDs of each parameter for multi-frequency combined inversion. The inversion results are represented by the vertical lines, whereas the MPDs are depicted by the curves. It can be seen from Fig. 3 that the upper sediment speed, sediment attenuation, basement speed, basement density and basement attenuation are reliable for multi-frequency combined inversion.

Frequency [Hz]	Layer	Thickness [m]	Speed [m/s]		Density [g/cm ³]	Attenuation [dB/λ]
			Upper	Lower		
Multi-frequency	Sediment	12.3725	1503.9	1613	1.1791	0.0941
	Basement		1696.6		1.9679	0.2842

Table 2: Inversion results for multi-frequency combined inversion.

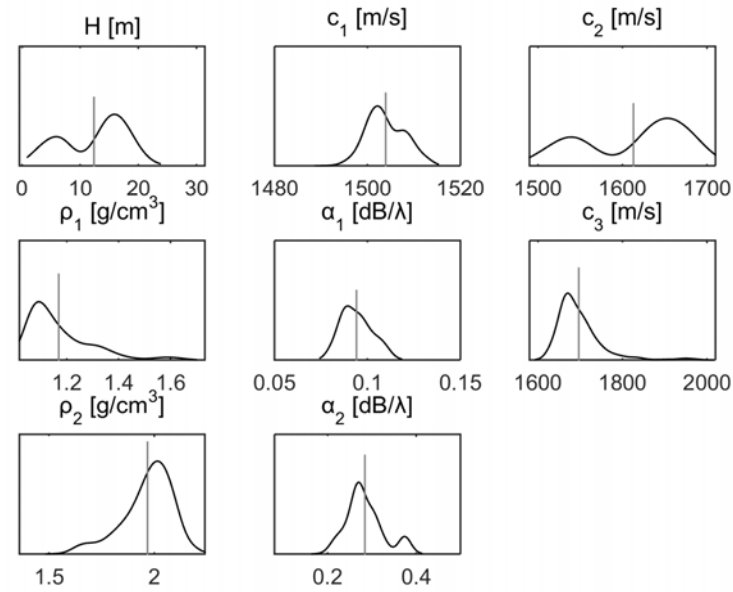


Fig.3: 1D MPDs of each parameter for multi-frequency combined inversion.

4. CONCLUSION

In summary, a new approach to estimating bottom parameters based on Bayesian theory in the deep ocean was presented in this paper. The wideband explosive sound source data from the SCS in the summer of 2014 were analyzed. This research obtained bottom parameters at varying frequencies while considering that the sensitivities of shallow-zone TLs vary for different frequencies of the bottom parameters in the deep ocean. Besides, this paper shows the inversion results for multi-frequency combined inversion. Through single frequency inversion and multi-frequency combined inversion, we can accurately obtain the bottom parameters.

REFERENCES

- [1] Yang K, Ma Y, Sun C, et al. Multistep matched-field inversion for broad-band data from ASIAEX2001. *IEEE Journal of Oceanic Engineering*, 29(4), pp.964, 2004.
- [2] Jiang Y M, Chapman N R, Badiy M. Quantifying the uncertainty of geoacoustic parameter estimates for the New Jersey shelf by inverting air gun data. *Journal of the Acoustical Society of America*, 121(4), pp.1879, 2007.
- [3] Potty G R, Miller J H, Lynch J F. Inversion for sediment geoacoustic properties at the New England Bight. *Journal of the Acoustical Society of America*, 114(4 Pt 1), pp.1874, 2003.
- [4] Bonnel J, Dosso S E, Ross C N. Bayesian geoacoustic inversion of single hydrophone light bulb data using warping dispersion analysis. *Journal of the Acoustical Society of America*, 134(1), pp.120, 2013.
- [5] Duan R, Ross Chapman N, Yang K, et al. Sequential inversion of modal data for sound attenuation in sediment at the New Jersey Shelf. *Journal of the Acoustical Society of America*, 139(1), pp.70, 2016.

- [6] Dosso S E. Quantifying uncertainty in geoacoustic inversion. I. A fast Gibbs sampler approach. *Journal of the Acoustical Society of America*, 111(1 Pt 1), pp.129, 2002.
- [7] Dosso S E, Nielsen P L. Quantifying uncertainty in geoacoustic inversion. II. Application to broadband, shallow-water data. *Journal of the Acoustical Society of America*, 111(1 Pt 1), pp.143, 2002.
- [8] Tarantola A. Inverse problem theory. Methods for data fitting and model parameter estimation. *Amsterdam Elsevier*, pp.615, 1987.
- [9] Sen M K, Stoffa P L. Bayesian inference, Gibbs' sampler and uncertainty estimation in geophysical inversion. *Geophysical Prospecting*, 44(2) pp.313, 2010.
- [10] Stoffa S . Global Optimization Methods in Geophysical Inversion. *Advances in Exploration Geophysics*, 4, 1995.